JOURNAL OF MATERIALS SCIENCE 27 (1992) 1397–1403

Effects of processing and valence states of metal oxides on electrical properties of ZnO varistors

YING-CHUNG CHEN, CHI-YEN SHEN, HONE-ZERN CHEN, YIN-FANG WEI
Institute of Electrical Engineering, National Sun Yat-Sen University, Kaohsiung, Taiwan
LONG WU
Department of Electrical Engineering, National Cheng Kung University, Tainan, Taiwan

The electrical characteristics of ZnO varistors with various valence states of manganese and cobalt were studied. The electrical properties of varistors are discussed in terms of defects produced by the additions. Compositions with lower trap densities have the characteristics of higher non-linear coefficient, higher voltage ratio and lower leakage current. The electrical properties are improved by increasing the sintering temperature and time due to a better tunnelling effect. It is also found that the depression angle and relaxation time decrease as a function of increasing sintering time, and the depression angle decreases and relaxation time increases with increasing sintering temperature. This indicates an enhancement in the degree of uniformity in trapping conductance and the trap emission/capture rate when the sintering time increases. The dependence of the depression angle and relaxation time on the composition are also presented.

1. Introduction

The zinc oxide varistors are polycrystalline devices composed mainly of ZnO with a few additions of other metal oxides such as Bi_2O_3, Sb_2O_3, CoO and MnO [1]. The microstructure of ZnO varistors consists of highly conductive zinc oxide grains surrounded by thin insulating grain boundaries which constitute double Schottky barriers, and Bi-rich phases appear between grains and spinel particles [2–7]. These Schottky barriers arise from the trapping of electrons and control the electrical characteristics of varistors. These trapped electrons are charge-compensated by positive shallow donors and donor-like traps located at the depletion regions of the grain boundaries [8]. The electron traps are majority carrier traps in ZnO varistors.

The charge trapping phenomena occur mainly in depletion regions of the grain boundaries and result in a.c. dispersion. The multiple trapping relaxations lead to a terminal capacitance. One of these relaxations of ZnO varistors is associated with the native/intrinsic defects within depletion regions of the grain boundaries [8–13]. Many investigators have made use of admittance spectroscopy, deep-level transient spectroscopy, etc. to observe the relaxation at $\simeq$ 100 KHz [8–12, 14, 15]. It has been shown that there is a dependence of the a.c. parameters on temperature, d.c. biasing, sintering temperature, and soaking time for the relaxation in the vicinity of 100 KHz [10, 13].

It is well known that the non-ohmic property of ZnO varistors is largely affected by the addition of metal oxides [16, 17], in which manganese and cobalt can enhance the non-linear coefficient of the varistor. However, the effect of valence states of additions on varistors, particularly on electrical properties, have not been clear till now. The traps produced by various valence states of additions are still not investigated. In this study, the various valence states of manganese and cobalt were employed in ZnO–Bi_2O_3-based varistors. The dependence of donor concentration, trap density and barrier height on the valence states of manganese and cobalt, as well as the variations of the relaxation in the vicinity of 100 KHz in the C* plane with sintering temperature and time, are studied. In addition, the types of trap resulting from various valence states of manganese and cobalt are analysed.

2. Experimental procedure

Four types of specimen were prepared in this study. The compositions are shown in Table I. The sintered samples were prepared by conventional ceramic fabrication techniques. Each composition was individually mixed by a stirrer with acetone to eliminate contamination by other impurities. After being dried and calcined at 700 °C for 2 h, the powders were ground by mortar and pestle and pressed into discs of 10 mm diameter and 1.7 mm thickness. These specimens were sintered at 1250 to 1280 °C in air with a soaking time of 1 to 2 h. Finally, some of the sintered samples were coated with conductive silver paint on both surfaces to provide an ohmic contact.

I–V measurements of these samples were made by using a d.c. power supply in a current range up to 1 A.

0022–2461

TABLE I Compositions of ZnO varistors used in this study

No.	Composition
S1	97 mol % ZnO + 0.5 mol % ($2Sb_2O_3$ + Cr_2O_3 + Bi_2O_3 + CoO + MnO)
S2	97 mol % ZnO + 0.5 mol % ($2Sb_2O_3$ + Cr_2O_3 + Bi_2O_3 + CoO + MnO_2)
S3	97 mol % ZnO + 0.5 mol % ($2Sb_2O_3$ + Cr_2O_3 + Bi_2O_3 + Co_2O_3 + MnO)
S4	97 mol % ZnO + 0.5 mol % ($2Sb_2O_3$ + Cr_2O_3 + Bi_2O_3 + Co_2O_3 + MnO_2)

The non-linear coefficient was calculated in the current range of 1 to 10 mA from the equation

$$\alpha = \frac{\log I_2 - \log I_1}{\log V_2 - \log V_1} \quad (1)$$

where V_1 and V_2 are the voltages at the currents I_1 and I_2, respectively. The leakage current was calculated at 80% of $V_{60\,\mu A}$. The electrical field response, also known as the voltage ratio, was calculated by using the electric fields corresponding to current densities of 20 $\mu A\ cm^{-2}$ and 1 $mA\ cm^{-2}$ obtained from I–V data. A modified $(1/C^2)$–V method using an LCR meter at 10 kHz was applied to obtain the donor concentration N_D, trap density N_T and barrier height ϕ [18].

The acquisition of two-probe a.c. small-signal electrical data covering the frequency range $10\ Hz \leqslant f \leqslant 40\ MHz$ was accomplished by an impedance analyser HP4194A controlled by a computer. The a.c. electrical data from analysing the complex capacitance plane (the C^* plane) show some influence on the a.c. dispersion over the same frequency range at room temperature. The non-Debye Cole–Cole [19] empirical relation can describe each semicircular relaxation in the C^* plane:

$$C^* = C_{\text{high frequency}} + \frac{C_i}{1 + (j\omega_i\tau_i)^{1-h_i}} \quad (2)$$

where h_i $(0 \leqslant h_i \leqslant 1)$ is the depression angle parameter of the ith relaxation. The parameter C_i denotes chord length and τ_i denotes the average time constant. It follows that $(\omega_i\tau_i)_{\text{peak}} = 1$ corresponds to the peak of the semicircular relaxation. The parameter $C_{\text{high frequency}}$ is expressed by the left intercept of each relaxation. Each relaxation may be represented as an individual lumped equivalent R–C series branch [20–22]. Therefore, in the vicinity of 100 KHz, the τ_3 relaxation can be described by the equation

$$\omega_3\tau_3 = \omega_3 R_3 C_3 = 1 \quad (3)$$

where ω_3 is the peak angular frequency, R_3 is the trapping resistance and C_3 is the trapping capacitance determined by the chord of the semicircle. The finite depression angle is defined when the centre of a semicircular relaxation lie below the X axis in a semicircular relaxation response. The depression angle related to τ_3 is denoted by θ_3.

The sintered samples without ohmic contacts, which were to be used in secondary ion mass spectroscopy (SIMS) measurements, were rinsed in acetone for 10 min and then cleaned in deionized water by ultrasonic stirring.

3. Results and discussion

The donor concentration, trap density and barrier height corresponding to various compositions are shown in Fig. 1. It indicates that the S1 composition has the lowest N_D, N_T and ϕ values while the S4 composition has the highest N_D, N_T and ϕ values for each sintering condition.

From the transition temperatures of various valence states of manganese and cobalt [23], it is known that Co^{2+} and Mn^{2+} ions are more stable than Mn^{4+} ions when the temperature is above 895 and 535 °C, respectively. So, most of the Co^{3+} or Mn^{4+} ions can transform into Co^{2+} or Mn^{2+} ions in the sintered body. However, the samples which were originally mixed with Mn^{4+} (MnO_2) and/or Co^{3+} (Co_2O_3) have higher Mn^{4+} and/or Co^{3+} ion concentrations than those originally mixed with Mn^{2+} (MnO) and/or Co^{2+} (CoO). Therefore, the S4 composition should contain higher Mn^{4+} and Co^{3+} ion concentrations, and the S1 composition should contain lower concentrations.

Matsuoka [24] and Inada [2] have shown that manganese exists in grains and spinel particles. However, Driear *et al.* [25] have proposed that manganese is primarily active in the grain boundaries of ZnO, though manganese also exists in both grains and spinels. They also mention that situations which place either manganese or cobalt in the higher valence state will decrease these cation fractions in zinc-rich grains, but that these cation fractions are increased when both are in the high valence state [25].

In this paper, we do not agree with the latter conclusion of Driear *et al.* We find that more high valence state cobalt ion exists in grains, but the distribution of high valence of state manganese ion is primarily concentrated in the grain boundaries when both MnO_2 and Co_2O_3 are added to ZnO varistors. SIMS measurement is used to prove our inference. In ZnO varistors, the area of grains is much larger, maybe several hundred times, than that of grain boundaries; so during SIMS measurements, the probability of the analysis point of the electron beam locating at grains would be much larger than for grain boundaries. Thus, we assume that the data from measured samples is the result of measuring in the grain region. In addition, the high intensity of Zn^{2+} and the absence of bismuth or antimony ion peaks in SIMS analysis also verify that the analysis "hole" is indeed situated at the grains of ZnO varistors, not at the spinel or pyrochlore second phases [24, 26, 27]. The results of SIMS measurements are shown in Fig. 2.

Table II shows the relative intensities of Co^{2+},

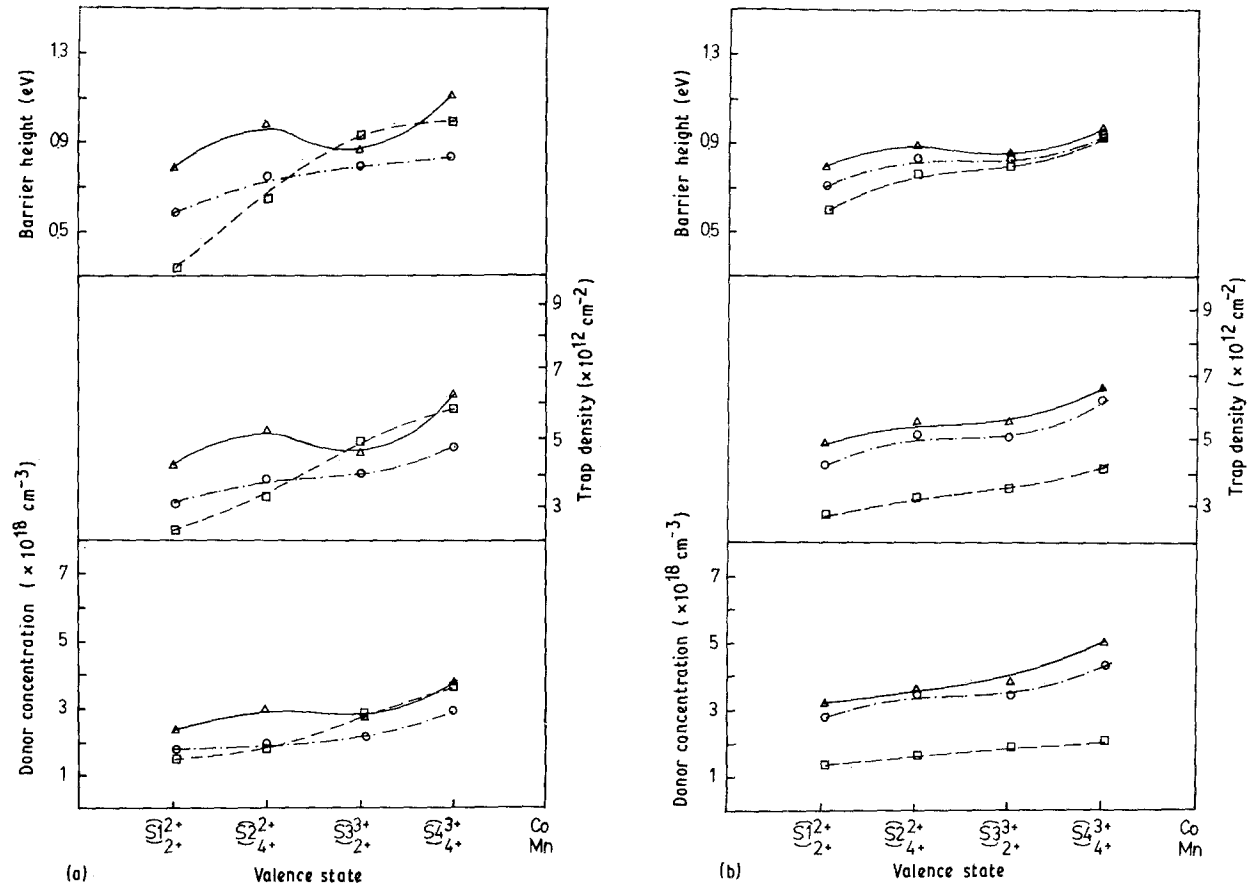

Figure 1 Donor concentration, trap density and barrier height of all samples for a sintering temperature of (a) 1250 °C and (b) 1280 °C. Sintering time (□) 1 h, (○) 1.5 h, (△) 2 h.

TABLE II Results of SIMS observed in a grain sintered at 1250 °C for 1 h

Ion	Relative intensity			
	S1	S2	S3	S4
Co^{2+}	8.5	22	1.3	11.3
Co^{3+}	0.09	0.1	0.09	0.8
Mn^{2+}	13	5.1	7.5	24.6
Mn^{4+}	2	3	1.5	0.7

Co^{3+}, Mn^{2+} and Mn^{4+} from four kinds of composition. It can be seen that the relative intensity of Mn^{4+} ions in grains of S1 composition, mixed with both manganese and cobalt in the low valence state, is higher than that of S4 composition, mixed with both manganese and cobalt in the high valence state. There would therefore be more remaining Mn^{4+} ions existing at grain boundaries in the S4 composition than in the S1 composition.

As mentioned above, in the S4 composition most of the Co^{2+} and Co^{3+} ions exist in the zinc-rich grains, while most of the Mn^{2+} ion, Mn^{4+} ion and some of the Co^{2+} ion exist near the grain boundaries. The Mn^{2+} and Co^{2+} ions can substitute for antimony ion and produce oxygen vacancy ($V_O^{\cdot\cdot}$) in depletion regions of the grain boundaries. The reactions followed [28] are

$$2MnO \rightarrow 2Mn'_{Sb} + V_O^{\cdot\cdot} + 2O_O^x \quad (4)$$

$$2CoO \rightarrow 2Co'_{Sb} + V_O^{\cdot\cdot} + 2O_O^x \quad (5)$$

At the same time, Mn^{4+} ion can substitute for antimony site and form antimony vacancy (V'''_{Sb}) near the grain boundaries. This reaction is described by

$$3MnO_2 \rightarrow 3Mn^{\cdot}_{Sb} + V'''_{Sb} + 6O_O^x \quad (6)$$

However, the Mn^{4+}, Mn^{2+} and Co^{2+} ions cannot substitute for bismuth ion in depletion regions of the grain boundaries, because the radii of these ions are much smaller than that of bismuth ion. It is inferred that there is a great number of oxygen vacancies and antimony vacancies appearing in the depletion regions of the grain boundaries and near the grain boundaries, respectively, in the S4 composition. On the other hand, the distribution of manganese and cobalt ions in the S1 composition is nearly the same as that in the S4 composition, except that Co^{2+} is replaced by Co^{3+} near the grain boundaries, and none of the oxygen vacancies can be produced by this replacement. The number of Mn^{4+} ions located at grain boundaries in the S1 composition is less than in the S4 composition, as obtained from the results of SIMS. So the numbers of $V_O^{\cdot\cdot}$ and V'''_{Sb} in the depletion regions of the grain boundaries and near the grain boundaries, respectively, in the S1 composition are less than in the S4 composition. It has been proved that oxygen vacancy is the intrinsic donor level of ZnO varistors [29]; and from the previous inference, the S4 composition contains higher donor concentrations and a higher barrier height owing to containing more $V_O^{\cdot\cdot}$ in the depletion

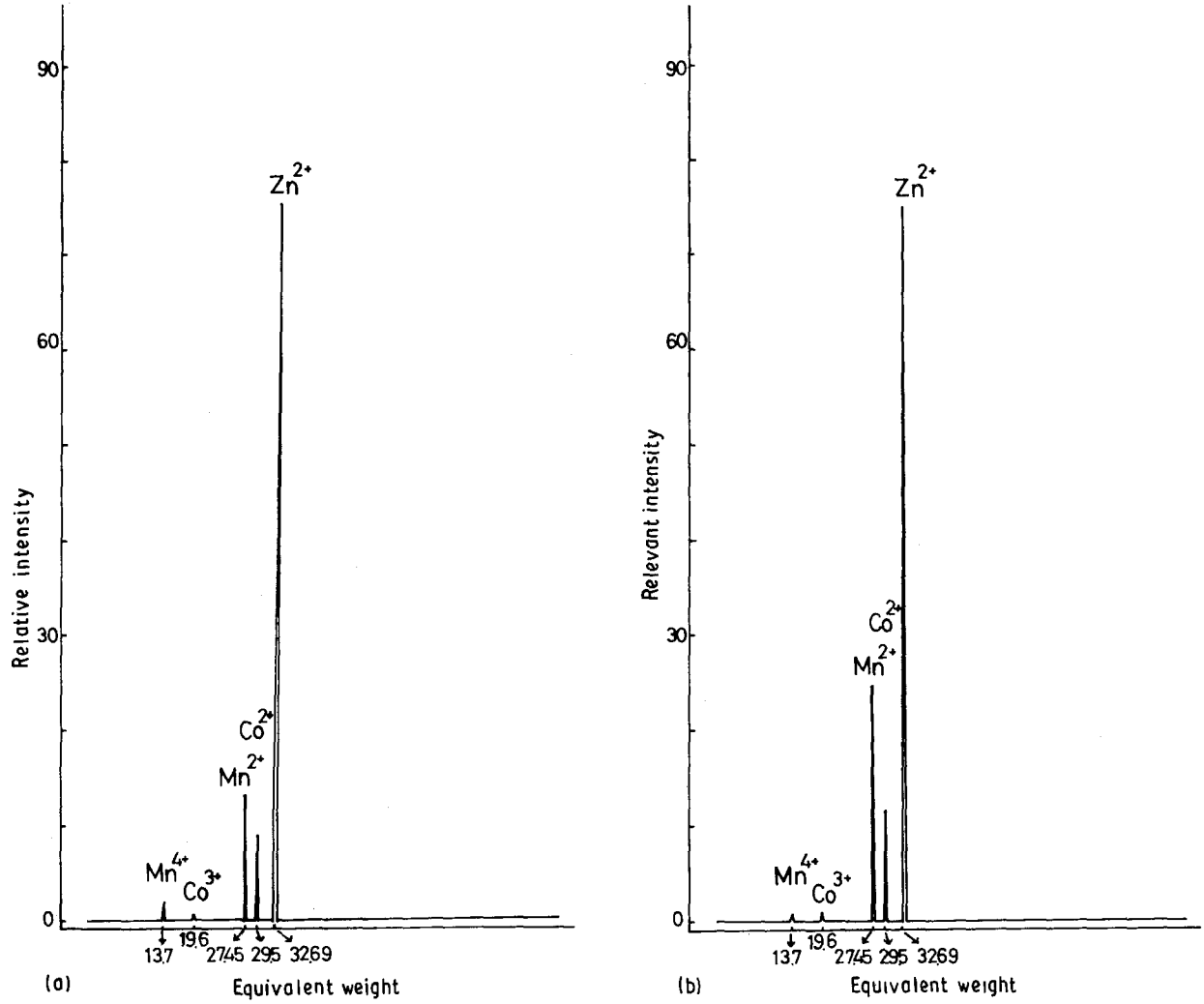

Figure 2 Results of SIMS for (a) S1 and (b) S4 with a measurement time of 40 min.

TABLE III Electrical properties of all samples

Sintering conditions		S1			S2			S3			S4		
Temp. (°C)	Time (h)	E^a	I_L (μA)	α	E^a	I_L (μA)	α	E^a	I_L (μA)	α	E^a	I_L (μA)	α
1250	1	0.37	25.8	34.7	0.20	28.6	30.8	0.34	29.2	18.6	0.21	28.6	14.5
	1.5	0.43	24.1	46.8	0.38	27.2	41.5	0.39	27.7	46.3	0.36	27.3	40.1
	2	0.47	22.9	48.7	0.39	26.6	44.2	0.44	23.4	47.5	0.39	26.7	41.5
1280	1	0.43	24.5	44.8	0.36	28.4	32.4	0.43	23.3	37.1	0.37	27.5	30.1
	1.5	0.48	21.6	46.8	0.42	25.1	34.8	0.46	23.1	41.6	0.41	26.1	31.0
	2	0.49	21.3	48.8	0.43	24.3	35.4	0.48	22.2	44.2	0.44	24.9	35.6

[a] $E = E_{20\,\mu A\,cm^{-2}}/E_{1\,mA\,cm^{-2}}$.

regions of the grain boundaries. In addition, there is a greater number of traps near the grain boundaries caused by V'''_{Sb}. With regard to the S1 composition which has lower donor concentrations, barrier height and trap density, this may be because of containing fewer $V_O^{\cdot\cdot}$ donor levels in the depletion regions and V'''_{Sb} traps near the grain boundaries.

The voltage ratio, leakage current (I_L) and non-linear coefficient (α) of all compositions are shown in Table III. It can be inferred from the data for the various compositions that the S1 composition has better electrical properties owing to its higher non-linear coefficient, higher voltage ratio and lower leakage current; thus the S1 composition yields improved non-linearity, a sharper knee region of the current–voltage response and a lower leakage current. This may be because of having a lower trap density within the S1 composition to contribute to conductance. All the same, the S1 composition possesses improvable electrical properties.

It can be seen from Table III that the electrical properties get better with increasing sintering temperature or time. This may be because the width of the grain boundaries decreases with increasing sintering

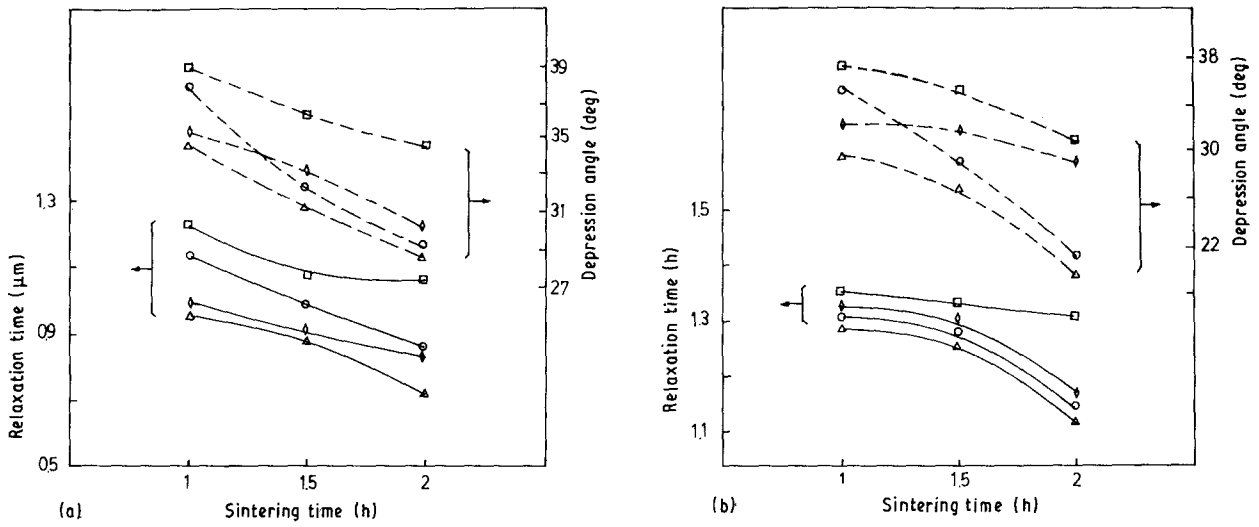

Figure 3 Room-temperature relaxation time and depression angle as a function of sintering time for samples sintered at (a) 1250 °C and (b) 1280 °C. (□) S1, (◇) S2, (○) S3, (△) S4.

TABLE IV Effects of sintering temperature and sintering time on room-temperature depression angle and relaxation time

Sintering conditions		S1		S2		S3		S4	
Temp (°C)	Time (h)	τ_3 (μs)	θ_3 (deg)	τ_3 (μs)	θ_3 (deg)	τ_3 (μs)	θ_3 (deg)	τ_3 (μs)	θ_3 (deg)
1250	1	1.22	38.5	0.99	35.0	1.14	37.5	0.96	34.5
1280	1	1.35	37.0	1.32	32.0	1.30	35.0	1.28	29.5
1250	1.5	1.08	36.0	0.91	33.0	0.98	32.0	0.88	31.0
1280	1.5	1.33	35.0	1.30	31.5	1.28	29.0	1.26	27.0
1250	2	1.06	34.5	0.84	30.0	0.85	29.0	0.73	28.5
1280	2	1.30	31.0	1.16	29.0	1.14	21.0	1.12	19.5

temperature or time. The tunnelling effect is apparent when the width of the boundaries decreases, and the electrical properties can improve. Improvement in the non-linear characteristic of the varistors by longer sintering time and higher sintering temperature is due to the wetting behaviour of the Bi_2O_3 intergranular phase [30]. The dihedral angle formed by the second phase at the grain boundary during sintering is zero, and the Bi_2O_3 liquid phase coats all the ZnO grains and dissolves a large amount of ZnO. During the cooling procedure, the dihedral angle becomes greater than zero and the Bi_2O_3 liquid phase recedes from the grain boundaries so that most of the ZnO grains are in direct contact. At the same time, the intergranular phase is stable at the multigrain junctions and forms a continuous three-dimensional network along the multigrain junctions. The Bi_2O_3 liquid phase does not need to wet all the grain boundaries in order to decrease the interface energy. This condition can be sufficient to produce good varistor electrical properties. In this study, a longer sintering time or higher sintering temperature can contribute to good ZnO–ZnO direct contacts and minimize the interface energy. So, these samples can exhibit better electrical properties.

The effects of sintering time on the depression angle (θ_3) and the relaxation time (τ_3) are shown in Fig. 3. The depression angle and the relaxation time decrease with increasing sintering time. This implies that spatial non-uniformity of intrinsic defects which existed near the boundary decreases with increasing sintering time. The more uniform distribution of intrinsic defects enhances the uniformity of trapping conductance. The relaxation time decreases with increasing sintering time, indicating that the trap emission/capture rate and the cross-section are enhanced. It is known from Table III that the longer is the sintering time, the better are the electrical properties. The nature of the conduction paths is a combination of the series–parallel non-uniform conducting network within the ZnO microstructure between the electrodes. A non-zero depression angle presents a degree of non-uniformity in the relaxation process between electrodes [31]. The decreasing depression angle indicates that the nature of non-uniformity in the relaxation process between the electrodes gradually unifies under the longer sintering time. This means that the conduction paths gradually approach a singular nature. Thus the electrical properties are better.

The relations between the depression angle and the relaxation time and various sintering conditions are illustrated in Table IV. The depression angle decreases and the relaxation time increases with increasing sintering temperature. This implies that the degree of uniformity in the trapping conductance is enhanced and the trap emission/capture rate is decreased when

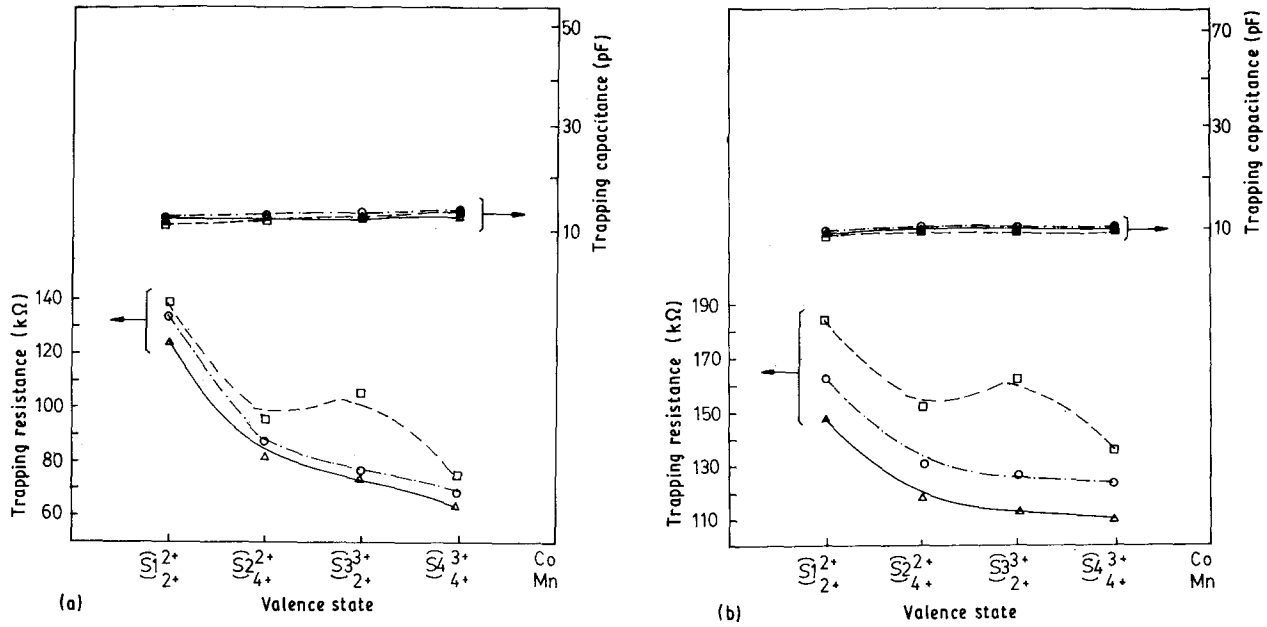

Figure 4 Room-temperature trapping resistance and trapping capacitance as a function of composition for samples sintered at (a) 1250 °C and (b) 1280 °C. Sintering time (□) 1 h, (○) 1.5 h, (△) 2 h.

sintering temperature is high. From Table III, it is found that the electrical properties are improved with increasing temperature. This is because the conduction paths between the electrodes gradually approach a singular nature, even if the relaxation time increases.

It can be observed from Fig. 3 and Table IV that the S4 composition possesses a smaller depression angle (θ_3) and relaxation time (τ_3), while the S1 composition possesses a larger depression angle and relaxation time. The relationships between composition and trapping resistance R_3 or trapping capacitance C_3 are shown in Fig. 4. It can be seen that the trapping capacitance is nearly constant for each composition. Therefore the trapping resistance is directly dependent on relaxation time. The S1 composition has a larger trapping resistance and contributes to a larger relaxation time and depression angle. In contrast, the S4 composition has a smaller trapping resistance so it possesses a smaller relaxation time and depression angle. The larger trapping resistance of the S1 composition is attributed to a lower donor concentration, whereas the smaller trapping resistance of the S4 composition is due to a higher donor concentration.

4. Conclusion

The electrical properties of ZnO varistors with various valence states of manganese and cobalt were investigated. The samples which originally contained high valence states of manganese and cobalt resulted in a high donor concentration, trap density and barrier height. This was due to higher $V_O^{\cdot\cdot}$ and $V_{Sb}^{'''}$ contents. The composition which originally contained low valence states of manganese and cobalt resulted in a lower donor concentration and trap density, owing to the lower $V_O^{\cdot\cdot}$ and $V_{Sb}^{'''}$ in it. From the electrical analysis, it can be concluded that samples with a lower trap density appear to have better electrical properties. The wetting behaviour of the intergranular phase also affects the electrical properties. A longer sintering time or higher sintering temperature makes most of the ZnO–ZnO junctions into direct contacts and minimizes the interface energy. For this reason the electrical properties become much better.

The depression angle and relaxation time decrease with increasing sintering time. It is concluded that the uniformity of trapping conductance, the trap emission/capture rate, and the cross-section are improved with an increase in sintering time. It is also found that a longer sintering time can gradually unify the nature of non-uniformity in the relaxation process between the electrodes. The depression angle decreases and the relaxation time increases with increasing sintering temperature. This implies that the degree of uniformity in the trapping conductance is enhanced when the sintering temperature increases. The samples containing a larger trapping resistance due to the lower donor concentration have a larger depression angle and relaxation time.

Acknowledgements

The authors wish to thank Miss H. R. Sze for technical assistance during SIMS measurement. Part of this work was supported by the National Science Council of the Republic of China under Contract No. NSC 80-0404-E-110-01.

References

1. M. MATSUOKA, *Jpn. J. Appl. Phys.* **10** (1971) 736.
2. M. INADA, *ibid.* **17** (1978) 1.
3. H. KANAI, M. IMAI and T. TAKAHASHI, *J. Mater. Sci.* **20** (1985) 3957.
4. E. OLSSON, L. K. L. FALK, G. L. DUNLOP and R. OSTERLUND, *ibid.* **20** (1985) 4091.
5. W. G. MORRIS, *J. Vac. Sci. Technol.* **13** (1976) 926.
6. D. R. CLARKE, *J. Appl. Phys.* **49** (1978) 2407.
7. A. T. SANTHANAM, T. K. GUPTA and W. G. CARLSON, *ibid.* **50** (1979) 852.

8. J. F. CORDARO, Y. SHIM and J. E. MAY, *ibid.* **60** (1986) 4186.
9. M. A. ALIM, M. A. SEITZ and R. W. HIRTHE, *ibid.* **63** (1988) 2337.
10. M. A. ALIM, *J. Amer. Ceram. Soc.* **72** (1989) 28.
11. Y. SHIM and J. F. CORDARO, *ibid.* **71** (1988) 184.
12. J. C. SIMPSON and J. F. CORDARO, *J. Appl. Phys.* **63** (1988) 1784.
13. L. C. SLETSON, M. E. POTTER and M. A. ALIM, *J. Amer. Ceram. Soc.* **71** (1988) 909.
14. N. SUOUATA, T. MATSUMUURA and T. OHNO, *Jpn. J. Appl. Phys.* **19** (1980) 1793.
15. A. NITAYAMA, H. SAKAKI and T. IKOMA, *ibid.* **19** (1980) L743.
16. A. KUSY and T. G. M. KLEINPENNING, *J. Appl. Phys.* **54** (1983) 2900.
17. K. KOUMOTO, K. AOKI and N. KITAORI, *Commun. Amer. Ceram. Soc.* **65** (1982) C-93.
18. K. MUKAE, K. TSUDA and I. NAGASAWA, *J. Appl. Phys.* **50** (1979) 4475.
19. R. H. COLE and K. S. COLE, *J. Chem. Phys.* **9** (1941) 341.
20. F. A. GRANT, *J. Appl. Phys.* **29** (1958) 76.
21. J. MASERJIAN, *J. Vac. Sci. Technol.* **6** (1976) 843.
22. D. H. EATON and C. T. SAH, *Solid-State Electron.* **16** (1973) 841.
23. "Handbook of Chemistry and Physics", 70th Edn (CRC, Florida, 1989–90) B-87.
24. M. MATSUOKA, in "Grain Boundary Phenomena in Electronic Ceramics", edited by L. M. Levinson (American Ceramic Society, Ohio, 1981) p. 190.
25. J. M. DRIEAR, J. P. GUEUTIN, T. O. SOKOLY and L. B. HACKNEY, *ibid.* p. 316.
26. C. W. NAN and P. N. ZHU, in "High Tech Ceramics", edited by P. Vincenzini (Elsevier Science, Amsterdam, 1987) p. 1825.
27. L. M. LEVINSON, "Advances in Varistor Technology", Ceramics Transactions Vol. 3 (American Ceramic Society, Westerville, 1989) p. 57.
28. Z. M. JARZEBSKI, "Oxide Semiconductors" (Pergamon, New York, 1973) p. 66.
29. G. D. MAHAN, *J. Appl. Phys.* **54** (1983) 3825.
30. J. P. GAMBINO, W. D. KINGERY, G. Z. PIKE, L. M. LEVINSON and H. R. PHILIPP, *J. Amer. Ceram. Soc.* **72** (1989) 642.
31. M. A. ALIM and M. A. SEITZ, *ibid.* **71** (1988) C-2469.

Received 16 January
and accepted 17 May 1991